Maxwell's Demon in the Ranque-Hilsch Vortex Tube

R. Liew,[1,*] J. C. H. Zeegers,[1] J. G. M. Kuerten,[2,3] and W. R. Michalek[2]

[1]Department of Applied Physics, Eindhoven University of Technology, P.O. Box 513, 5600 MB, Eindhoven, Netherlands
[2]Department of Mechanical Engineering, Eindhoven University of Technology, P.O. Box 513, 5600 MB, Eindhoven, Netherlands
[3]Faculty EEMCS, University of Twente, P.O. Box 217, 7500 AE Enschede, Netherlands

(Received 6 January 2012; published 1 August 2012)

A theory was developed that explains energy separation in a vortex tube, known as one of the Maxwellian demons. It appears that there is a unique relation between the pressures in the exits of the vortex tube and its temperatures. Experimental results show that the computed and measured temperatures are in very good agreement.

DOI: 10.1103/PhysRevLett.109.054503 PACS numbers: 47.32.Ef, 47.27.T−, 47.40.Hg

Energy separation by tangentially injecting pressurized gas into a cylindrical tube, from which the gas is allowed to escape from both ends, was first discovered by Ranque [1] and improved by Hilsch [2]. The device they invented has the common name "vortex tube" or Ranque-Hilsch Vortex Tube (RHVT). The RHVT consists of a cylindrical tube, which has typically a length to diameter ratio of 20–50, connected to the so-called vortex chamber to which one or more entrance nozzles are connected as shown in Fig. 1. Pressurized gas is expanded through the nozzles to generate a highly swirling motion. Located near the nozzles there is an opening (cold exit), which has a smaller diameter than the tube, from which part of the gas leaves the system at lower temperature. The remaining gas exits the other side of the tube, the hot exit, and has a higher temperature. The ratio of cold and total mass flow ($\dot{m}_c$ and $\dot{m}$ respectively) is the so-called cold fraction $\varepsilon = \frac{\dot{m}_c}{\dot{m}}$, which is usually controlled by a control valve at the hot end side of the tube. Simplicity, durability (no moving parts), the small size, and instantly available cold air make the RHVT popular at places where pressurized air is available to generate (spot-) cooling, e.g., for the machining of plastic and to cool electronics [3–5].

One of the main questions in literature of the last decades was (see, for example, Refs. [2,6–17]) what causes the energy separation process in the RHVT? Although all existing theories give ideas of possible process(es) inside the RHVT, it appears that quantitative comparison of the existing theories with experiments is very difficult. Hilsch [2] was the first who explained energy separation by means of internal friction that causes energy transport from the core to the peripheral region, making gas in the core region to cool down, while heating up the gas in the peripheral region. Schultz-Grunow [9] explained that a difference in potential temperature between the core and periphery results in radial energy transport. Deissler and Perlmutter [6] obtained mathematical results and concluded that shear work is the main source of the energy separation. Linderstrom-Lang [7] developed an incompressible model and concluded that turbulent transfer of thermal energy is the cause of the energy separation. Ahlborn *et al.* [13] have developed a model that predicts the energy separation by means of a heat pump in the vortex tube. Although their model is semi-incompressible and one dimensional, it predicts the phenomenon with reasonable accuracy.

In the developed theories, the inlet and cold exit pressures are often used as (important) parameters. The hot exit pressure, however, was neglected so far. In this Letter, we introduce a simple compressible model in which the hot exit pressure appears to be important as well. Experiments were performed to validate the model, leaving a robust method to predict energy separation with the RHVT at high accuracy.

Since the invention of the RHVT, people find the device mysterious and unexplainable. Maybe the so-called Maxwell demon is present in the device that separates cold and hot molecules from each other, creating the temperature difference. The RHVT is nowadays often mentioned while giving examples of such Maxwellian demons.

To understand why energy transfer exists, we provide the following example, which is based on existing theories [6,9,13]: Imagine an infinitely long cylinder filled with gas that rotates at an angular velocity Ω [Fig. 2(a)]. The radial component of the momentum balance shows that there exists a radial pressure gradient due to the centrifugal force. The pressure p at the axis is therefore lower than the pressure near the cylinder wall [Fig. 2(b)]. In the absence of radial motions, the energy equation shows that the static temperature of the gas is constant.

If one moves a gas pocket from the axis towards the cylinder wall [$1 \rightarrow 2$ in Fig. 2(a)], however, the pressure of the gas pocket increases due to compression. If this

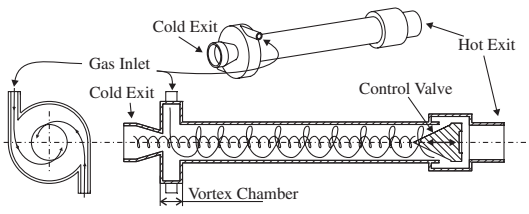

FIG. 1. The Ranque-Hilsch vortex tube.

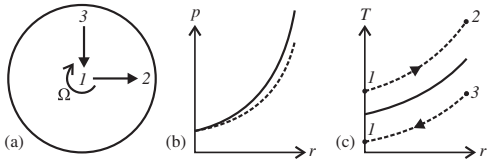

FIG. 2. Rotating cylinder with radial flow. (a) Rotating cylinder filled with gas. (b) Pressure as a function of the radial coordinate. (c) Temperature as a function of the radial coordinate. The solid lines in the middle and right figure show adiabatic conditions.

compression is fast and without heat exchange between the gas pocket and its surroundings, the compression is adiabatic and the temperature of the gas pocket increases [Fig. 2(c)]. Therefore, at point 2, the gas pocket has a higher temperature than its surroundings. The other way around, if one moves a gas pocket adiabatically from the cylinder wall towards the axis ($3 \rightarrow 1$) the gas pocket is expanded and obtains a lower temperature than its surroundings. After compression or expansion, energy is exchanged between the gas pocket and its surrounding gas. This heat exchange process includes, among others, conduction, diffusion, and mainly turbulent mixing [6,7,13]. The (turbulent) heat exchange process heats up the peripheral region while cooling down the core region and only exists in the presence of radial velocity fluctuations.

Because of the adiabatic compression or expansion of gas pockets, the pressure p and temperature T are related according to

$$T \sim p^{\gamma-1/\gamma}, \tag{1}$$

where $\gamma = \frac{c_p}{c_v}$ is the adiabatic exponent and is the ratio between the specific heat capacities at constant pressure c_p and constant volume c_v. Because the pressure in the core is lower than in the peripheral region, the temperature in the core region is lower than gas located near the walls. Consequently, gas that is extracted from the core region has a lower temperature than gas that is extracted from the peripheral region: Maxwell's demon is revealed.

In the RHVT, the process is similar as described above [13], where the compression and expansion stages of gas pockets are caused by turbulent eddies [6]. Examples of flow patterns in vortex tubes that show turbulent eddies are given by Refs. [18–20]. Instead of one large heat pump [13], each eddy pumps heat from the core towards the periphery. During this process, the temperature differences between the compressed or expanded gas pockets with their surroundings diminish while heat is transported [6]. At some point (in space and time), the limit of (static) temperature separation is reached [indicated with the solid lines in Figs. 2(b) and 2(c)], provided that there is enough time, i.e., the RHVT is long enough. This explains why there is an optimal length of the RHVT: too short and this limit is not reached; too long and the limit is reached, but because of the longer tube, losses (e.g., convective heat losses to the surroundings) negatively influence the performance.

In literature, Eq. (1) is mainly used to determine inflow conditions or the thermodynamic efficiency of the RHVT [2,11,14]. The explanation of why we end up with this relation may be simple; however, no attempt was made so far to compute the cold and hot exit temperatures by making direct use of this equation.

The average pressure ratio of the compression and expansion stages in the RHVT is found by dividing the hot exit pressure p_{ht} by the cold exit pressure p_{ct}. Subscripts h (hot) and c (cold) are used to distinguish the hot and the cold fluid properties respectively, pl denotes plenum properties, and subscript t is used to indicate stagnation (total) properties. Due to adiabatic deceleration of fluid that moves towards the hot exit in the peripheral region, the kinetic energy of the fluid is converted into heat [13], additional to the heat transferred by the eddies. The total temperature ratio between the exits can then be computed with

$$\frac{T_{ht}}{T_{ct}} = \left(\frac{p_{ht}}{p_{ct}}\right)^{\gamma-1/\gamma}\left(1 + \frac{\gamma-1}{2}\,\mathrm{Ma}_0^2\right), \tag{2}$$

where the first term on the right-hand side is the temperature ratio due to compression or expansion, and last term, containing the maximum swirl Mach number (Ma_0, found at $r = R_{vt}$ with R_{vt},is the vortex tube radius), contributes for the adiabatic deceleration (where only the swirl component has a significant contribution). The Mach number is defined as the velocity of the gas divided by the local speed of sound. The proposed model is valid as long as there are radial velocity fluctuations. In the absence of these radial motions, there will be no compression or expansion of gas pockets and, consequently, no energy separation.

While gas expands through the RHVT, no work and (approximately no) heat is extracted from it. According to the first law of thermodynamics, the total enthalpy going into the system h_{pl}, equals the sum of the total enthalpy at the hot exit h_{ht} and at the cold exit h_{ct}, each times the flow fraction [$(1-\varepsilon)$ or ε, respectively] of gas leaving that exit:

$$h_{\mathrm{pl}} = \varepsilon h_{ct} + (1-\varepsilon)h_{ht}. \tag{3}$$

For a perfect gas, the total enthalpy can be written as a function of the temperature $h_t = c_p T_t$, and the exit temperatures are found as functions of T_{pl} (the plenum temperature), p_{ht}/p_{ct}, ε, γ, and Ma_0.

If the RHVT has a vortex chamber, Ma_0 is generally not known. However, it can be found as a function of the plenum pressure p_{pl} and p_c by making use of the isentropic gas relations that apply in the entrance nozzles. Experimental results of the swirl Mach number inside the vortex chamber that we have measured with a cylindrical type pitot tube, or CPT (more about this method is found in Refs. [12,21]) are shown with symbols in Fig. 3. This figure shows the measured Mach number as a function of the

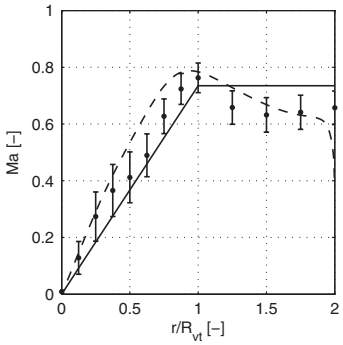

FIG. 3. Swirl Mach number as a function of the radial coordinate, measured with a cylindrical type pitot tube. The symbols are *CPT* results, the dotted line is the result of a RANS simulation, and the solid line is the simplified model.

radial coordinate (r/R_{vt}) compared to results of a numerical simulation (Fluent^{TM}, RANS $k-\varepsilon$ model) that we have performed (shown as the dotted line). The most simple approximation of Ma(r) is shown as the solid line in the figure: solid body rotation in the core (also seen in [16]); Ma(r) is constant in the outer region.

If we use the approximated velocity in the radial component of the momentum equation, while taking into account that the static temperature is constant in the vortex chamber and neglecting the viscosity, the pressure ratio between inlet and cold exit becomes

$$\frac{p_{\mathrm{pl}}}{p_c} = \exp\left(\frac{\gamma}{2}\mathrm{Ma}_0^2\right)\left(\frac{R_{vc}}{R_{vt}}\right)^{\gamma \mathrm{Ma}_0^2}\left(1+\frac{\gamma-1}{2}\mathrm{Ma}_0^2\right)^{\gamma/\gamma-1}, \quad (4)$$

where R_{vc} is the radius of the vortex chamber. The solid line in Fig. 3 was constructed with Ma_0 found by using this equation and the measured p_{pl} and p_c. Note that Ma_0 is located at $r = R_{vt}$ and that the agreement with the *CPT* result at this radius is fairly good.

To verify that the static temperature is constant in the vortex chamber, we have performed experiments on a RHVT over a wide range of cold fractions ($0.05 \leq \varepsilon \leq 0.95$) and mass flows ($\dot{m} = 35$–$80$ g/s). More details of the experiments follow later. By using Eq. (4), we computed the Ma_0, which was then used to determine the static temperature ($T_{R_{vt}}$) at $r = R_{vt}$. The static cold exit temperature T_c was found by applying 1D compressible gas dynamics where we have used the measured T_{ct}, p_{ct}, and ε. The average ratio is $T_c/T_{R_{vt}} = 1.01$ with a deviation of 1.7%, showing that the static temperature in the vortex chamber is indeed approximately constant.

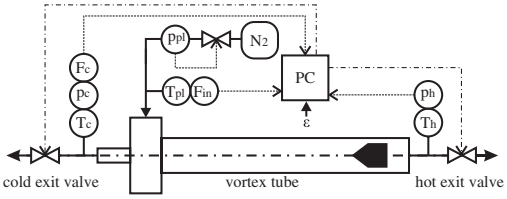

FIG. 4. Schematic overview of the experimental setup.

Experiments were performed with nitrogen gas to show the unique relation between pressure and temperature in the RHVT. The RHVT was insulated and had a radius of $R_{vt} = 0.02$ m and a length of 2.25 m. The vortex chamber had a radius of $R_{vc} = 0.04$ m and contained 8 rectangular (1×14 mm) entrance nozzles. A schematic overview of the experimental setup is shown in Fig. 4. The plenum pressure p_{pl} was controlled via a pressure controller that was connected to the nitrogen tank N_2 and remained constant during an experiment. The inlet mass flow $\dot{m}$ was measured via mass flow sensor F_{in} and was used together with the cold mass flow sensor F_c (both have an error less than 1% FS) to regulate the two exit valves to obtain the set value for ε. The temperatures were recorded with $pt1000$ temperature probes (accuracy of 0.01 K), and the pressures were measured with digital pressure sensors [accuracy of 0.02% FS (0–21 bar)]. All temperatures, pressures, and mass flows were recorded simultaneously.

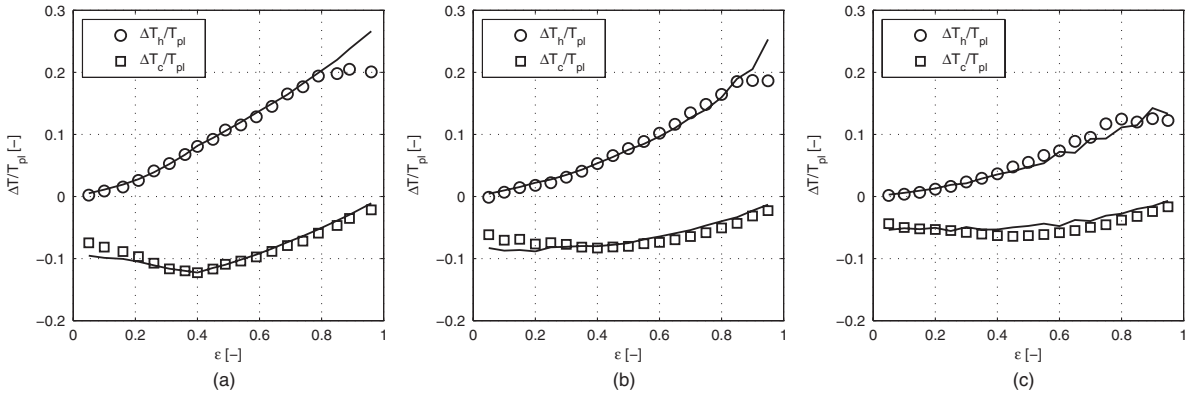

FIG. 5. Dimensionless temperature differences as a function of ε. Symbols are measurement results, the solid lines are computed with Eq. (2). (a) Maximum mass flow ($\dot{m}$ = variable) at $p_{\mathrm{pl}} = 4.70$ bar. (b) Constant mass flow ($\dot{m} = 65.3$ g/s). (c) Constant mass flow ($\dot{m} = 35.3$ g/s). The absolute error in the experimental values is less than 0.005. Error bars are not shown because of their negligible sizes.

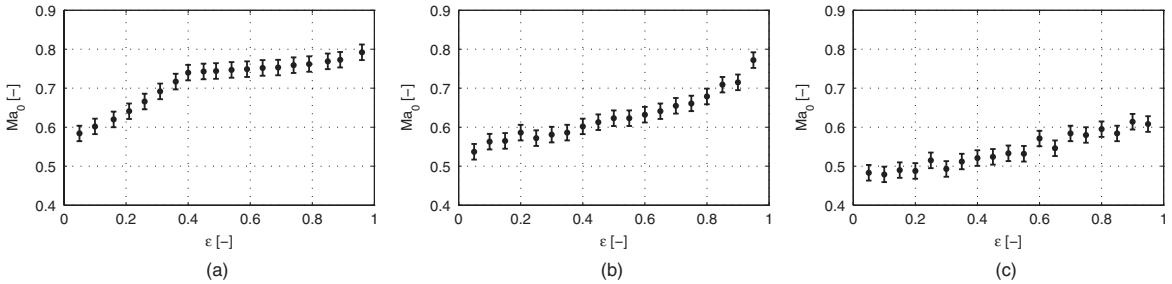

FIG. 6. Maximum swirl Mach number computed with Eq. (4) as a function of ε. (a) Maximum mass flow ($\dot{m}$ = variable) at $p_{\mathrm{pl}} = 4.70$ bar. (b) Constant mass flow ($\dot{m} = 65.3$ g/s). (c) Constant mass flow ($\dot{m} = 35.3$ g/s).

The exit temperatures are made dimensionless with T_{pl} and are shown in Fig. 5 where ΔT is the difference between the exit and inlet temperature. The symbols are measured quantities, and the solid lines are the predicted values according to Eqs. (2)–(4). The results shown in Fig. 5(a) were obtained from an experiment where the exit valves were controlled to give the maximum possible mass flow for each cold fraction while keeping p_{pl} fixed. The results shown in Fig. 5(b) were obtained with a constant mass flow of 65.3 g/s, and the results shown in Fig. 5(c) with 35.3 g/s. The differences between the modeled and experimental values for $\Delta T_h/T_{\mathrm{pl}}$ at larger cold fractions are caused by heat losses to the surroundings. Although the net heat loss is relatively small, the relative drop in T_{ht} becomes larger as $\varepsilon \rightarrow 1$ because the amount of hot gas flowing through the hot exit becomes less and less. Because of the enthalpy balance, Eq. (3), any error in the model or experiment results in an increased deviation from the modeled with experimental values as $\varepsilon \rightarrow 0$.

The corresponding Mach numbers are shown in Fig. 6. In the experiment where the mass flow was kept maximum, Ma_0 is a nondifferentiable function [Fig. 6(a)] of ε due to the varying mass flow. For a constant mass flow through the system, ε can only be increased by lowering the cold exit pressure. According to Eq. (4), a decreasing cold exit pressure results in an increasing Ma_0. This is indeed observed from Figs. 6(b) and 6(c). In this Letter, we show the results of only three experiments. However, we have repeated the experiments over a wide range of cold fractions, ($\varepsilon = 0.05$–0.95), mass flows ($\dot{m} = 35$–80 g/s), and inlet pressures ($p_{\mathrm{pl}} = 2.75$–4.80 bar), all showing good agreement between the theory and experiments. The average error between the modeled and experimental values is only 1.1% (or 3.2 K absolute), illustrating the wide range of validity of the theory presented here.

In summary, we provide a theory that explains the energy separation process in the RHVT. Based on this theory, we have developed a model that only requires the inlet and exit pressures of the RHVT to be known, which predicts the temperatures at the hot and cold exit. To validate the model presented in this article, several experiments were performed. The temperatures computed with the model are in very good agreement with the measured values, showing that there is a unique relation between pressure and temperature in the RHVT, revealing Maxwell's demon.

The authors would like to thank Professor A. Hirschberg for his comments regarding energy transport by large eddies. This research is supported by the Dutch Technology Foundation STW, which is the applied science division of NWO, and the Technology Programme of the Ministry of Economic Affairs.

*r.liew@tue.nl

[1] M. G. Ranque, J. Phys. Radium **7**, 112 (1933).
[2] R. Hilsch, Rev. Sci. Instrum. **18**, 108 (1947).
[3] Exair, http://www.exair.com (2012).
[4] ITW-Vortec, www.vortec.com (2012).
[5] AirTx, http://www.airtx.com/vortex-tubes (2012).
[6] R. G. Deissler and M. Perlmutter, Int. J. Heat Mass Transfer **1**, 173 (1960).
[7] C. U. Linderstrom-Lang, J. Fluid Mech. **45**, 161 (1971).
[8] S. Eiamsa-ard and P. Promvonge, Renew. Sustain. Energ. Rev. **12**, 1822 (2008).
[9] F. Schultz-Grunow, Forsch. Ing. Wes. **17**, 65 (1951).
[10] K. Stephan, S. Lin, M. Durst, F. Huang, and D. Seher, Int. J. Heat Mass Transfer **26**, 341 (1983).
[11] A. Gutsol, Phys. Usp. **40**, 639 (1997).
[12] B. K. Ahlborn and S. Groves, Fluid Dyn. Res. **21**, 73 (1997).
[13] B. K. Ahlborn, J. U. Keller, and E. Rebhan, J. Non-Equilib. Thermodyn. **23**, 159 (1998).
[14] B. K. Ahlborn, J. U. Keller, R. Staudt, G. Treitz, and E. Rebhan, J. Phys. D **27**, 480 (1994).
[15] V. N. Shtern and A. A. Borissov, Phys. Fluids **22**, 083601 (2010).
[16] C. M. Gao, K. J. Bosschaart, J. C. H. Zeegers, and A. T. M. de Waele, Cryogenics **45**, 173 (2005).
[17] N. F. Aljuwayhel, G. F. Nellis, and S. A. Klein, Int. J. Refrig. **28**, 442 (2005).
[18] A. Secchiaroli, R. Ricci, S. Montelpare, and A. D'Alessandro, Int. J. Heat Mass Transfer **52**, 5496 (2009).
[19] T. Farouk, B. Farouk, and A. Gutsol, Int. J. Heat Mass Transfer **52**, 3320 (2009).
[20] Y. Xue, M. Arjomandi, and R. Kelso, Exp. Therm. Fluid. Sci. **35**, 1514 (2011).
[21] C. M. Gao, Ph.D. thesis, Eindhoven University of Technology (2005).